LOCAL CONVERGENCE OF AN EM-LIKE IMAGE RECONSTRUCTION METHOD FOR DIFFUSE OPTICAL TOMOGRAPHY*

Caifang Wang

College of Art and Sciences, Shanghai Maritime University, Shanghai 200135, China
LMAM, School of Mathematical Sciences, Peking University, Beijing 100871, China
Email: wangcfg@gmail.com

Tie Zhou

LMAM, School of Mathematical Sciences, Peking University, Beijing 100871, China
Email: tzhou@math.pku.edu.cn

Abstract

In this paper, an EM-like image reconstruction iterative formula specifically developed for stable external sources is rewritten as a map towards a fixed point iteration. Local convergence of the image reconstruction method is then proved. Finally a three-dimensional numerical image reconstruction example is presented.

Mathematics subject classification: 78A70, 78M50, 93B15.
Key words: Diffuse optical tomography, Image reconstruction, Fixed-point iteration, Local convergence.

1. Introduction

Diffuse optical tomography (DOT) is an optical imaging modality, which provides the spatial distribution of the optical parameters inside a random media [1]. This nondestructive technique has advantage of directly measuring the physiologically relevant tissue and blood oxygenation, and is now widely used in breast cancer diagnostics [2,3], joint imaging [4] and blood oximetry in human muscle and brain tissues [5,6].

In DOT, the near-infared external sources are used to delivery the light signals. The intensity and path-length distributions of the exiting photons provide information about the optical properties of the transilluminated tissue by means of a physical models of the light migration. The propagation of light in highly scattering media, such as biological tissue may be described by the radiative transfer equation (RTE) [7]. When the medium is predominantly scattering rather than absorption, the diffusion approximation (DA) is a good approach to the RTE, away from sources and boundaries and it has been widely used in DOT [7,8].

Mathematically, the image reconstruction of DOT is an inverse problem solving the absorption and diffusion coefficient from the boundary measurements. Various reconstruction methods based on DA model have been established. The analytical methods with different boundary conditions are studied in a series of papers [9–11] and they can reconstruct optical parameters only in simple region cases. The iterative optimization based reconstruction methods [12] are used widely since they can deal with optical parameters in complex regions. In

these methods, the problem is regarded as the optimization of an objective function representing the sum-squared difference of the data to the model, plus additional regularization terms representing prior knowledge. An EM-like reconstruction method for stationary sources DOT is proposed, see, e.g., [13]. In this method, the boundary measurements are assumed to have independent and identical Poisson distributions. The problem is regarded as the optimization of a log-likelihood function with nonnegative constrain of optical parameters.

In this paper, we investigate the convergence of the EM-like image reconstruction which is specifically developed for stable external sources condition. The rest of the paper is organized as follows. In Section 2, we review the photon migration model and introduce the stationary sources DOT forward and inverse problems. In Section 3 we derive the EM-like image reconstruction algorithm. In Section 4, the local convergence of this algorithm is proved. In Section 5, a 3-D numerical example is presented.

2. DOT Forward and Inverse Problems

Let $\Omega \subset \mathbb{R}^3$ be a domain that contains the tissue to be imaged, bounded by surface $\Gamma = \partial\Omega$. Let $\mu_a(x)$ and $\mu_s(x)$ be the absorption and scattering coefficients of the tissue, respectively. Denote $D(x)$ as the diffusion coefficient which is expressed as

$$D(x) = \frac{1}{3(\mu_a(x) + \mu_s'(x))}, \tag{2.1}$$

where $\mu_s' = (1 - \bar{\eta})\mu_s$ is the reduced scattering coefficient of the media and $\bar{\eta}$ is an anisotropy factor ($0 \le \bar{\eta} \le 1$).

We consider the cases in which the tissue to be imaged is illuminated by multiple stationary external sources. Denote S as the number of external sources. Under each irradiation, the measurement can be collected on part of the surface $\Gamma_i \subset \Gamma$, $i = 1, \cdots, S$.

Individual photons from the stationary external source migrate through the tissue and undergo many scattering events or absorption events according to the local values of the tissue's optical parameters. Each photon may either have negligible contribution, or escape from the surface $\partial\Omega$, thus contributing to the boundary measurements. Under each irradiation, the macroscopic phenomena of photons can be described with a steady state diffusion equation (DA model)

$$-\nabla \cdot (D(x)\nabla u_i(x)) + \mu_a(x)u_i(x) = 0, \qquad x \in \Omega, \tag{2.2}$$

where $u_i(x)$ is the isotropic photon density inside Ω for $i = 1, \cdots, S$. The external source information is contained in the boundary condition

$$u_i(x) + 2AD(x)\frac{\partial u_i}{\partial \nu}(x) = g_i^-(x), \qquad x \in \Gamma, \tag{2.3}$$

where $g_i^-(x)$ is the total inward flux, A is a parameter that describes the mismatch between the refractive index within Ω and the refractive index in the surrounding medium [14, 15], ν is the exterior normal. The steady-state attenuation measurements are collected on part of the surface $\Gamma_i \subset \Gamma$, $i = 1, \cdots, S$, and can be defined as the outward flux

$$g_i(x) = -D\frac{\partial u_i}{\partial \nu}(x), \qquad x \in \Gamma_i, \quad i = 1, \cdots, S. \tag{2.4}$$

We use a vector

$$g = (g_1, \cdots, g_S)^{\mathrm{T}} \tag{2.5}$$

to represent the group of boundary measurements.

If the boundary measurements are known, the Robin boundary condition (2.3) on Γ_i can be replaced with Dirichlet boundary condition

$$u_i(x) = g_i^-(x) + 2A g_i(x), \quad x \in \Gamma_i. \tag{2.6}$$

With the boundary condition and boundary measurements, the DOT problem is to solve the optical parameters $\mu_a(x)$ and $D(x)$ with the corresponding diffusion approximation u_i, ($i = 1, \cdots, S$) such that

$$
\begin{cases}
-\nabla \cdot (D(x)\nabla u_i(x)) + \mu_a(x)u_i(x) = 0, & x \in \Omega, \\
u_i(x) + 2AD\dfrac{\partial u_i}{\partial \nu}(x) = g_i^-(x), & x \in \Gamma, \\
D\dfrac{\partial u_i}{\partial \nu}(x) = -g_i(x), & x \in \Gamma_i.
\end{cases}
\tag{2.7}
$$

or

$$
\begin{cases}
-\nabla \cdot (D(x)\nabla u_i(x)) + \mu_a(x)u_i(x) = 0, & x \in \Omega, \\
u_i(x) + 2AD\dfrac{\partial u_i}{\partial \nu}(x) = g_i^-(x), & x \in \Gamma \setminus \Gamma_i, \\
u_i(x) = g_i^-(x) + 2A g_i(x), & x \in \Gamma_i, \\
D\dfrac{\partial u_i}{\partial \nu}(x) = -g_i(x), & x \in \Gamma_i.
\end{cases}
\tag{2.8}
$$

Since u_i can be determined by the following mixed boundary value problems (MBVPs):

$$
\mathrm{DOT(P)}
\begin{cases}
-\nabla \cdot (D(x)\nabla u_i(x)) + \mu_a(x)u_i(x) = 0, & x \in \Omega, & i = 0, \cdots, S, \\
u_i(x) + 2AD\dfrac{\partial u_i}{\partial \nu}(x) = g_i^-(x), & x \in \Gamma \setminus \Gamma_i, & i = 0, \cdots, S, \\
u_i(x) = g_i^-(x) + 2A g_i(x), & x \in \Gamma_i, & i = 0, \cdots, S.
\end{cases}
\tag{2.9}
$$

We define a DOT forward operator $\mathcal{F}_i[\mu_a, D] : L^2(\Omega) \times L^2(\Omega) \to H^{-1/2}(\Gamma_i)$ as follows

$$\mathcal{F}_i[\mu_a, D] = -D \left.\frac{\partial u_i}{\partial \nu}\right|_{\Gamma_i}, \qquad i = 0, \cdots, S, \tag{2.10}$$

where u_i is the solution of the MBVP (2.9). Therefore the forward problem of DOT can be expressed as

$$g = \mathcal{F}[\mu_a, D], \tag{2.11}$$

where

$$\mathcal{F} = (\mathcal{F}_1, \mathcal{F}_2, \cdots, \mathcal{F}_S)^{\mathrm{T}}. \tag{2.12}$$

Assume that the boundary measurements are of independent and identical Poisson distributions. Similarly to the formulation in [20], we define a log-likelihood function

$$\Phi[\mu_a, D] = \sum_{i=1}^{S} \int_{\Gamma_i} \left\{ g_i \log \mathcal{F}_i[\mu_a, D] - \mathcal{F}_i[\mu_a, D] \right\} d\Gamma. \tag{2.13}$$

With maximum likelihood estimation (MLE) method in statistics, the inverse problem of DOT can be defined as the optimization of the log-likelihood function

$$\arg \max_{\mu_a \geq 0, D > 0} \Phi[\mu_a, D]. \tag{2.14}$$

3. EM-Like Image Reconstruction Algorithm

To solve the optimization problem, the Fréchet derivative of the objective function should be considered. Let $\Phi'[\mu_a, D] = (\Phi'_{\mu_a}[\mu_a, D], \Phi'_D[\mu_a, D])$ be the Fréchet derivative of $\Phi[\mu_a, D]$. According to [13],

$$\Phi'[\mu_a, D] = \left(-\sum_{i=1}^{S} (\psi_i - \phi_i) u_i, \ -\sum_{i=1}^{S} \nabla(\psi_i - \phi_i) \cdot \nabla u_i \right), \tag{3.1}$$

where u_i is the solution to (2.9), and ψ_i and ϕ_i satisfy

$$\begin{cases} -\nabla \cdot (D\nabla\psi_i) + \mu_a \psi_i = 0, & \text{in } \Omega, \\ \psi_i + 2AD\dfrac{\partial\psi_i}{\partial\nu} = 0, & \text{on } \Gamma \setminus \Gamma_i, \\ \psi_i = \dfrac{g_i}{\mathcal{F}_i[\mu_a, D]}, & \text{on } \Gamma_i, \end{cases} \tag{3.2}$$

and

$$\begin{cases} -\nabla \cdot (D\nabla\phi_i) + \mu_a \phi_i = 0, & \text{in } \Omega, \\ \phi_i + 2AD\dfrac{\partial\phi_i}{\partial\nu} = 0, & \text{on } \Gamma \setminus \Gamma_i, \\ \phi_i = 1, & \text{on } \Gamma_i, \end{cases} \tag{3.3}$$

respectively. With the Kuhn-Tucker condition [16] in the following:

$$\exists\, \mu_0(x), \mu_1(x), \mu_2(x) \geq 0, \quad \mu_0(x)^2 + \mu_1(x)^2 + \mu_2(x)^2 \neq 0, \qquad \text{for } x \in \Omega, \tag{3.4}$$

such that

$$\mu_0(x)\Phi'_D\big[\mu_a(x), D(x)\big] + \mu_1(x) = 0, \tag{3.5a}$$

$$\mu_0(x)\Phi'_{\mu_a}\big[\mu_a(x), D(x)\big] + \mu_2(x) = 0, \tag{3.5b}$$

and

$$\mu_1(x)D(x) = 0, \qquad \mu_2(x)\mu_a(x) = 0, \tag{3.6}$$

we arrive at

$$\mu_a(x)\Phi'_{\mu_a}\big[\mu_a(x), D(x)\big] = 0, \tag{3.7a}$$

$$D(x)\Phi'_D\big[\mu_a(x), D(x)\big] = 0. \tag{3.7b}$$

Equivalently, we have

$$\mu_a \sum_{i=1}^{S} \psi_i u_i = \mu_a \sum_{i=1}^{S} \phi_i u_i, \tag{3.8a}$$

$$D \sum_{i=1}^{S} \nabla\psi_i \cdot \nabla u_i = D \sum_{i=1}^{S} \nabla\phi_i \cdot \nabla u_i. \tag{3.8b}$$

Therefore the following iterative formulas can be used to update the diffusion coefficients and absorption coefficients:

$$\mu_a^{(n+1)} = \mu_a^{(n)} \frac{\sum_{i=1}^{S} \phi_i^{(n)} u_i^{(n)}}{\sum_{i=1}^{S} \psi_i^{(n)} u_i^{(n)}}, \tag{3.9a}$$

$$D^{(n+1)} = D^{(n)} \frac{\sum_{i=1}^{S} \nabla\psi_i^{(n)} \cdot \nabla u_i^{(n)}}{\sum_{i=1}^{S} \nabla\phi_i^{(n)} \cdot \nabla u_i^{(n)}}. \tag{3.9b}$$

From the iterative formulas, the optical parameters might overshoot at one step, then in the next step, the value of forward operator $\mathcal{F}_i$ might be negative and ψ_i would be negative afterwards. When the optical parameters are overshooting, we have to roll back to the previous step and add a positive constant to the third equation of (3.2) and (3.3).

4. Convergence Analysis

To simplify the notations, we denote

$$p = (\mu_a, D) \in L^2(\Omega) \times L^2(\Omega), \tag{4.1}$$

as a pair of real-valued optical parameters. We analyze the behavior of iterative formulas (3.9a) and (3.9b) in a neighborhood of the maximum point p^*. According to the properties of the log-likelihood function, p^* exists and occurs in the interior of the feasible region. Rewrite the iterative formulas (3.9b) and (3.9a) as

$$p^{(n+1)} = p^{(n)} + \mathcal{C}[p^{(n)}] \cdot \Phi'[p^{(n)}], \tag{4.2}$$

where

$$\mathcal{C}[p] = \left(\frac{\mu_a}{\sum_{i=1}^{S} \psi_i u_i}, \frac{-D}{\sum_{i=1}^{S} \nabla \phi_i \cdot \nabla u_i} \right). \tag{4.3}$$

We can view the iterations given by (4.2) as a map moving toward a fixed point

$$\mathcal{G}[p] = p + \mathcal{C}[p] \cdot \Phi'[p]. \tag{4.4}$$

To analyze the convergence of the iterative formulas (3.9a) and (3.9b) for image reconstruction of DOT, we need the following lemmas.

Lemma 4.1. ([17,18]) *Let $\mathcal{X}$ be a Banach space, $\mathcal{A}$ a smooth (nonlinear) operator in $\mathcal{X}$ with fixed point x^*, and $\mathcal{A}'$ the Fréchet derivative of the operator $\mathcal{A}$. The fixed point x^* may be obtained as the limit*

$$x^* = \lim_{n \to \infty} x_n,$$

where x_n is given by the successive approximations

$$x_{n+1} = \mathcal{A}x_n \quad (n = 0, 1, \cdots)$$

for any initial value x_0 sufficiently close to x^*, provided that the spectral radius of the Fréchet derivative $\mathcal{A}'(x^*)$ of $\mathcal{A}$ at x^* is strictly less than 1.

Lemma 4.2. *Assume that operators $\mathcal{A} : \mathcal{X} \to \mathcal{X}$ and $\mathcal{B} : \mathcal{X} \to \mathcal{X}$ are positive definite, $\mathcal{A} - \mathcal{B} : \mathcal{X} \to \mathcal{X}$ is non-negative definite. Then the spectral radius of the operator $\mathcal{A}^{-1}(\mathcal{A} - \mathcal{B}) : \mathcal{X} \to \mathcal{X}$ lies on $[0, 1)$.*

Proof. Let λ be the eigenvalue of operator $\mathcal{A}^{-1}(\mathcal{A} - \mathcal{B}) : \mathcal{X} \to \mathcal{X}$ and $\xi \in \mathcal{X}$ be the corresponding eigenfunction. We have

$$\mathcal{A}^{-1}(\mathcal{A} - \mathcal{B})\xi = \lambda \xi, \tag{4.5}$$

which gives

$$(\mathcal{A} - \mathcal{B})\xi = \lambda \mathcal{A}\xi, \tag{4.6}$$

Let $\mathcal{K} = \mathcal{A} - \mathcal{B}$. Then $\mathcal{A} = \mathcal{K} + \mathcal{B}$, which yields

$$(1 - \lambda)\mathcal{K}\xi = \lambda \mathcal{B}\xi. \tag{4.7}$$

The inner product of ξ and the above equation in $\mathcal{X}$ is

$$\langle (1 - \lambda)\mathcal{K}\xi, \xi \rangle_{\mathcal{X}} = \langle \lambda \mathcal{B}\xi, \xi \rangle_{\mathcal{X}}, \tag{4.8}$$

i.e.

$$(1 - \lambda)\langle \mathcal{K}\xi, \xi \rangle_{\mathcal{X}} = \lambda \langle \mathcal{B}\xi, \xi \rangle_{\mathcal{X}}. \tag{4.9}$$

Since the operators $\mathcal{B}$ is positive definite and $\mathcal{K}$ is non-negative definite, we have $(1 - \lambda)\lambda > 0$ or $\lambda = 0$. Then $0 \le \lambda < 1$. Hence the spectral radius of the operator $\mathcal{A}^{-1}(\mathcal{A} - \mathcal{B})$ lies on $[0, 1)$. This completes the proof. $\qquad\square$

The following lemma is about the Fréchet derivative of the forward operator $\mathcal{F}_i$, ($i = 1, \cdots, S$).

Lemma 4.3. ([13, 19]) *Consider the MBVPs (2.9). Let* $p = (D, \mu_a)$ *be a pair of real functions defined in* $L^2(\Omega) \times L^2(\Omega)$, *which satisfies*

$$0 < m_D \le D(x) \le M_D, \qquad 0 \le \mu_a(x) \le M_\mu, \tag{4.10}$$

where $m_D, M_D, M_\mu > 0$. *Let* $h = (h_D, h_{\mu_a})$ *be a pair of bounded functions defined in* $L^2(\Omega) \times L^2(\Omega)$, *and* $h_D = 0$ *on* Γ. *Then the Fréchet derivative of the forward operator is defined as*

$$\mathcal{D}\mathcal{F}_i h = -D\frac{\partial v_i}{\partial \nu}, \qquad on \ \Gamma_i, \tag{4.11}$$

where v_i *is the solution of the following MBVP*

$$\begin{cases} -\nabla \cdot (D\nabla v_i) + \mu_a v_i = \nabla \cdot (h_D \nabla u_i) - h_{\mu_a} u_i, & in \ \Omega, \\ v_i + 2AD\dfrac{\partial v_i}{\partial \nu} = 0, & on \ \Gamma \setminus \Gamma_i, \\ v_i = 0, & on \ \Gamma_i. \end{cases} \tag{4.12}$$

Lemma 4.4. *Let* $h = (h_D, h_{\mu_a})$ *be a pair of bounded function defined in* $L^2(\Omega) \times L^2(\Omega)$, $h_D = 0$ *on the boundary* Γ, *and* Φ *be the log-likelihood function defined in Eq. (2.13). Let* $p^* = (D^*, \mu_a^*)$ *be the extremum point of* $\Phi[p]$. *Then the second Fréchet derivative of* $\Phi[p]$ *at* p^* *is*

$$\mathcal{D}^2\Phi[p^*]h^2 = \sum_{i=1}^{S} \int_{\Gamma_i} \frac{-g_i}{\mathcal{F}_i^2[p^*]} \left(-D^*\frac{\partial v_i^*}{\partial \nu} \right)^2 \mathrm{d}\Gamma, \tag{4.13}$$

where v_i^* *is the solution of MBVP (4.12) with the optical parameters* p^*.

Proof. Let

$$f(t) = \Phi[p^* + th], \qquad for \ t \sim 0. \tag{4.14}$$

Direct calculations give

$$
\begin{aligned}
\left.\frac{\mathrm{d}^2}{\mathrm{d}t^2}f(t)\right|_{t=0} &= \frac{\mathrm{d}}{\mathrm{d}t}\sum_{i=1}^{S}\int_{\Gamma_i}\left\{g_i\frac{1}{\mathcal{F}_i[p^*+th]}-1\right\}\frac{\mathrm{d}}{\mathrm{d}t}\mathcal{F}_i[p^*+th]\mathrm{d}\Gamma\bigg|_{t=0} \\
&= \sum_{i=1}^{S}\int_{\Gamma_i}\frac{-g_i}{\mathcal{F}_i^2[p^*]}\left(\frac{\mathrm{d}}{\mathrm{d}t}\mathcal{F}_i[p^*+th]\right)^2\bigg|_{t=0}\mathrm{d}\Gamma + \sum_{i=1}^{S}\int_{\Gamma_i}\left(\frac{g_i}{\mathcal{F}_i[p^*]}-1\right)\frac{\mathrm{d}^2}{\mathrm{d}t^2}\mathcal{F}_i[p^*+th]\bigg|_{t=0}\mathrm{d}\Gamma \\
&= \sum_{i=1}^{S}\int_{\Gamma_i}\frac{-g_i}{\mathcal{F}_i^2[p^*]}\left(-D^*\frac{\partial v_i^*}{\partial\nu}\right)^2\mathrm{d}\Gamma + \sum_{i=1}^{S}\int_{\Gamma_i}\left(\frac{g_i}{\mathcal{F}_i[p^*]}-1\right)\frac{\mathrm{d}^2}{\mathrm{d}t^2}\mathcal{F}_i[p^*+th]\bigg|_{t=0}\mathrm{d}\Gamma. \quad (4.15)
\end{aligned}
$$

Since we have

$$
\Phi'[p^*]=0, \tag{4.16}
$$

on the extrumum point p^* and according to Eq. (3.1), we obtain

$$
g_i = \mathcal{F}_i[p^*]. \tag{4.17}
$$

Finally we arrive at

$$
\left.\frac{\mathrm{d}^2}{\mathrm{d}t^2}f(t)\right|_{t=0} = \sum_{i=1}^{S}\int_{\Gamma_i}\frac{-g_i}{\mathcal{F}_i^2[p^*]}\left(-D\frac{\partial v_i^*}{\partial\nu}\right)^2\mathrm{d}\Gamma. \tag{4.18}
$$

This completes the proof of the lemma.   □

It follows from Lemma 4.1 that the fixed point p^* of (4.4) is locally attractive provided that the spectral radius of the differential $\mathrm{d}\mathcal{G}$ is strictly less than 1. In the following, we estimate the spectral radius of $\mathrm{d}\mathcal{G}$ and give the convergence analysis of the reconstruction method.

Since $\Phi'[p^*]=0$, we have

$$
\begin{aligned}
\mathrm{d}\mathcal{G}[p^*] &= I + \mathcal{C}[p^*]\mathcal{D}^2\Phi[p^*] \\
&= \mathcal{C}[p^*]\left(\mathcal{C}^{-1}[p^*]+\mathcal{D}^2\Phi[p^*]\right), \tag{4.19}
\end{aligned}
$$

where $\mathcal{D}^2\Phi[p^*]$ represents the second Fréchet derivative. According to Lemma 4.2, when $\mathcal{C}^{-1}[p^*]$ and $-\mathcal{D}^2\Phi[p^*]$ are positive definite, $\mathcal{C}^{-1}[p^*]+\mathcal{D}^2\Phi[p^*]$ is non-negative definite. Consequently, the spectral radius of $\mathrm{d}\mathcal{G}$ is strictly less than 1.

Consider the following MBVPs

$$
\begin{cases}
-\nabla\cdot(D\nabla v_i)+\mu_a v_i = q_i, & \text{in }\Omega, & i=1,\cdots,S, \\
v_i+2AD\dfrac{\partial v_i}{\partial\nu}=0, & \text{on }\Gamma\setminus\Gamma_i, & i=1,\cdots,S, \\
v_i=0, & \text{on }\Gamma_i. & i=1,\cdots,S.
\end{cases} \tag{4.20}
$$

Define linear bounded operators $\Lambda_i:L^2(\Omega)\to\Gamma_i$ as [20]

$$
\Lambda_i[q_i]=-D\frac{\partial v_i}{\partial\nu}. \tag{4.21}
$$

Let $\|\Lambda_i\|=T_i$. Let C be the constant that satisfies

$$
\|\nabla\cdot(\xi_2\nabla u_i)\|\le C\|\xi_2,\nabla u_i\|, \qquad \forall\xi=(\xi_1,\xi_2)\in L^2(\Omega)\times L^2(\Omega), \quad \xi\not\equiv 0.
$$

Theorem 4.1. *For $i = 1, \cdots, S$, let $g_{i,\min} = \min_{x \in \Gamma_i} g_i(x)$, $p^* = (D^*, \mu_a^*)$ be the pair of optical parameters in extremum point. The iterative reconstruction method* (3.9) *is local convergent if the following properties are satisfied*

$$\phi_i \geq g_{i,\min}^{-1} T_i^2 \mu_a^* u_i, \tag{4.22}$$

$$-\nabla u_i \cdot \nabla \phi_i \geq g_{i,\min}^{-1} T_i^2 C^2 D^* \nabla u_i \cdot \nabla u_i, \tag{4.23}$$

where C and T_i are the constants defined above.

Proof. We analyze the convergence of the reconstruction method for absorption and diffusion coefficients, respectively. For the iteration of absorption coefficient, we have

$$\langle -\mathcal{D}_{\mu_a}^2 \Phi[p^*] \xi_1, \xi_1 \rangle_{L^2(\Omega)} = -\mathcal{D}_{\mu_a}^2 \Phi[p^*] \xi_1^2 = \sum_{i=1}^{S} \int_{\Gamma_i} g_i^{-1} \Lambda_i^2 [-\xi_1 u_i] \mathrm{d}\Gamma > 0, \tag{4.24}$$

$$\langle \mathcal{C}_{\mu_a}^{-1}[p^*] \xi_1, \xi_1 \rangle_{L^2(\Omega)} = \int_\Omega \frac{\sum_{i=1}^{S} u_i \psi_i}{\mu_a} \xi_1^2 \mathrm{d}x = \sum_{i=1}^{S} \int_\Omega \frac{u_i \phi_i}{\mu_a} \xi_1^2 \mathrm{d}x > 0 \tag{4.25}$$

where in the second last step we have used the fact $\psi = \phi$ at p^*. Moreover, we have

$$\langle (\mathcal{C}_{\mu_a}^{-1}[p^*] + \mathcal{D}_{\mu_a}^2[p^*]) \xi_1, \xi_1 \rangle_{L^2(\Omega)}$$

$$= \sum_{i=1}^{S} \left(\int_\Omega \frac{u_i \phi_i}{\mu_a} \xi_1^2 \mathrm{d}x - \int_{\Gamma_i} g_i^{-1} \Lambda_i^2 [u_i \xi_1] \mathrm{d}\Gamma \right)$$

$$\geq \sum_{i=1}^{S} \int_\Omega \left(\frac{u_i \phi_i}{\mu_a} \xi_1^2 - g_{i,\min}^{-1} T_i^2 u_i^2 \xi_1^2 \right) \mathrm{d}x$$

$$= \sum_{i=1}^{S} \int_\Omega u_i \xi_1^2 \left(\frac{\phi_i}{\mu_a} - g_{i,\min}^{-1} T_i^2 u_i \right) \mathrm{d}x \geq 0. \tag{4.26}$$

It follows from Lemma 4.2 that the spectral radius of operator $\mathrm{d}\mathcal{G}[p^*]_{\mu_a}$ is strictly less than 1. For the iteration of diffusion coefficient, we have

$$\langle -\mathcal{D}_D^2 \Phi[p^*] \xi_2, \xi_2 \rangle_{L^2(\Omega)} = -\mathcal{D}_D^2 \Phi[p^*] \xi_2^2 = \sum_{i=1}^{S} \int_{\Gamma_i} g_i^{-1} \Lambda_i^2 [\nabla \cdot (\xi_2 \nabla u_i)] \mathrm{d}\Gamma > 0. \tag{4.27}$$

For $i = 1, \cdots, S$, u_i and ϕ_i are the solution to two different MBVPs with external sources at different boundary, hence we have $\nabla u_i \cdot \nabla \phi_i < 0$. It follows that

$$\langle \mathcal{C}_D^{-1}[p^*] \xi_2, \xi_2 \rangle_{L^2(\Omega)} = \int_\Omega \frac{\sum_{i=1}^{S} \nabla u_i \cdot \nabla \phi_i}{-D} \xi_2^2 \mathrm{d}x = \sum_{i=1}^{S} \int_\Omega \frac{\nabla u_i \cdot \nabla \phi_i}{-D} \xi_2^2 \mathrm{d}x > 0, \tag{4.28}$$

and

$$\langle (\mathcal{C}_D^{-1}[p^*] + \mathcal{D}_D^2[p^*]) \xi_2, \xi_2 \rangle_{L^2(\Omega)}$$

$$= \sum_{i=1}^{S} \left(\int_\Omega \frac{\nabla u_i \cdot \nabla \phi_i}{-D} \xi_2^2 \mathrm{d}x - \int_{\Gamma_i} g_i^{-1} \Lambda_i^2 [-\nabla \cdot (\xi_2 \nabla u_i)] \mathrm{d}\Gamma \right)$$

$$\geq \sum_{i=1}^{S} \int_\Omega \left(\frac{\nabla u_i \cdot \nabla \phi_i}{-D} \xi_2^2 - g_{i,\min}^{-1} T_i^2 (-\nabla \cdot (\xi_2 \nabla u_i))^2 \right) \mathrm{d}x$$

$$\geq \sum_{i=1}^{S} \int_{\Omega} \left(\frac{\nabla u_i \cdot \nabla \phi_i}{-D} \xi_2^2 - g_{i,\min}^{-1} T_i^2 C^2 \xi_2^2 \nabla u_i \cdot \nabla u_i \right) \mathrm{d}x$$

$$= \sum_{i=1}^{S} \int_{\Omega} \xi_2^2 \left(\frac{\nabla u_i \cdot \nabla \phi_i}{-D} - g_{i,\min}^{-1} T_i^2 C^2 \nabla u_i \cdot \nabla u_i \right) \mathrm{d}x \geq 0. \qquad (4.29)$$

According to Lemma 4.2, the spectral radius of operator $\mathrm{d}\mathcal{G}[p^*]_D$ is strictly less than 1. $\qquad \square$

Remark 4.1. When the conditions (4.22) and (4.23) in Theorem 4.1 are not satisfied, the local convergence may be obtained by modifying the boundary conditions (3.2) and (3.3) to

$$\psi_i = \frac{g_i}{\mathcal{F}_i[p]} + c, \qquad \text{on } \Gamma_i,$$
$$\phi_i = 1 + c, \qquad \text{on } \Gamma_i.$$

If the constant c is sufficiently large, the conditions (4.22) and (4.23) still hold.

5. Numerical Example

We use a 3-D numerical experiment to test the performance of the reconstruction algorithm. The reconstruction is implemented on an IBM laptop T60(Intel (R) Core(TM)2 CPU T7200 2.00GHz with 2.00GB RAM) and the operator system is Ubuntu 7.10 with GNU compiler GCC4.0. All the elliptic boundary value problems are solved with the finite element package AFEPack (`http://dsec.pku.edu.cn/~rli/software_e.php`).

The phantom used here is a cylinder with height 30 mm and radius 15 mm. Inside the cylinder, there are three cylinders with height 3 mm and radius 5 mm. The center of the three cylinders are (0,0,6) mm, (0,0,0) mm and (0,0,-6) mm, respectively. The optical parameters of the phantom are list in Table 5.1. All the optical parameters chosen here are similar to the optical parameters of mouse's lung (L), heart (H) and muscle (M) tissues (NIR 500 nm-800 nm), respectively [21]. The appearance of the phantom is show in Fig. 5.1.

Assume that the experiment is taken in a black circumstance and no photon travels into the tissue except for the external sources. We set 40 sources on the side of the cylinder. The position of the sources on the expanded diagram of cylinder is in Fig. 5.2. The boundary measurements are assumed to be detected on half of the cylinder's side opposite to the current source. Boundary measurements are calculated from Eq. (2.4) and re-sampled in the resolution of 159×101 with a grid size of 0.3 mm. Since the finite element method is used to solve the forward problem in the experiment, the boundary measurements are corrupted by the approximation error [22,23] caused by sparse meshes although extra noises are not added.

Table 5.1: Information of the phantom.

Region	center [mm]	μ_a [mm^{-1}]	μ_s [mm^{-1}]
1 (L)	(0,0,6)	0.023	2.000
2 (H)	(0,0,0)	0.011	1.096
3 (L)	(0,0,-6)	0.023	2.000
background (M)	(0,0,0)	0.007	1.031

Fig. 5.1. The numerical phantom.
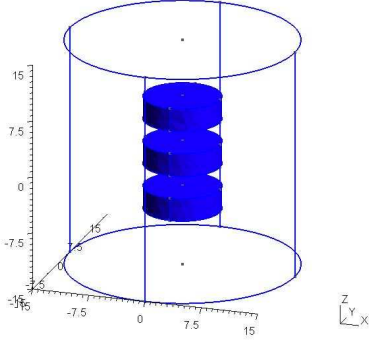

Fig. 5.2. Position of sources.

The phantom is a cylinder of 30 mm height and 30 mm diameter centered at $(0,0,0)$ mm. The small cylinders inside the phantom are with the radius 5 mm and are at $(0,0,6)$ mm, $(0,0,0)$ mm and $(0,0,-6)$ mm, respectively.

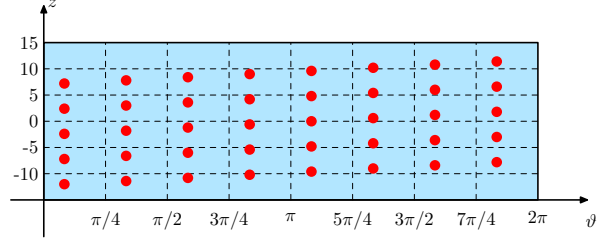For the i-th source $(i = 1, \cdots, S)$, the center of the source is $(R\cos\vartheta_0, R\sin\vartheta_0, z)$, where R is the radius of the cylinder, ϑ_0 and z satisfy

$$\begin{cases} z = -12 + 0.6(i - 1), \\ \vartheta_0 = \pi/12 + \text{mod } (i - 1, 8) \cdot \pi/4. \end{cases}$$
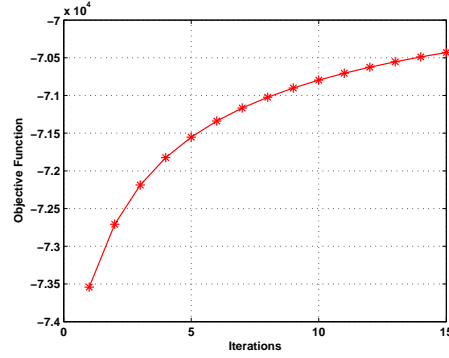
Fig. 5.3. The value of objective function is plotted against the iterations.

We assume that the internal structure of the phantom is known and the optical parameters are piecewise constant. The iteration is started with the optical parameters $(0.015,0.25)\text{mm}^{-1}$, $(0.007,0.3211)\text{mm}^{-1}$ and $(0.015,0.25)\text{mm}^{-1}$ in three different regions, respectively. The iteration is set to be a constant. The iterative formulas in (3.9) are for the updating of optical parameters on different points. With the prior of information of the regions, the reconstruction procedure is to determine the value of the optical parameters in different regions. During each iteration, the optical parameters in different regions are updated by integration on the region and followed by division. To avoid overshooting of optical parameters, we add a constant which equals to the iteration number plus 1 to the third equation of Eqs. (3.2) and (3.3).

The value of objective function in each iteration is shown in Fig. 5.3. The relative error of the absorption coefficient and diffusion coefficient of the three regions are shown in Fig. 5.4.

From Fig. 5.4, we find that the relative error of the absorption coefficients first decreases and after several iterations, it begins to increase. For the small cylinder centered at the origin,

the diffusion coefficient is close to the diffusion coefficient of the background, the relative error between the two coefficients is less than 7%. It approximates to the computation error of the underlying PDEs. Hence we can not get a reasonable solution of this region (cf. the second figure of Fig. 5.4). When the diffusion coefficient is fixed, we only reconstruct the absorption coefficient. With the same setting of the previous numerical experiment, we get the value of objective function and the relative error of absorption coefficient in each iteration (see Fig. 5.5). From Fig. 5.5, we find that the value of objective function and relative error of absorption coefficient in each iteration is similar in this numerical experiment and the previous one.

The semi-convergence phenomenon [24, 25] occurs in both numerical experiments. However, this phenomenon is not contrary to the convergence of the reconstruction algorithm due to the initial guess of optical parameters and the non-uniqueness of the problem. To reduce the semi-convergence behavior, we have to find a proper initial value of the optical parameters and stopping rule or specify perturbation parameters during iteration. Moreover, the accuracy of the PDE solvers should be increased so as to obtain reasonable solutions of the DOT. These will be considered in future works.
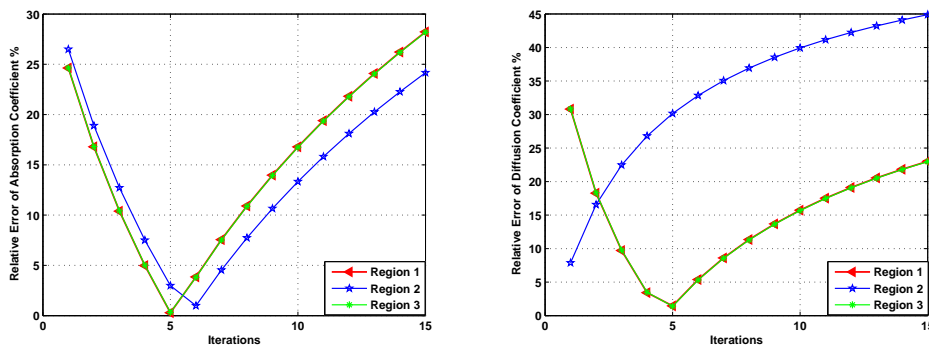

Fig. 5.4. The relative error of absorption and diffusion coefficients plotted against the iteration. Left: the relative error of absorption coefficient and right: the relative error of diffusion coefficient.
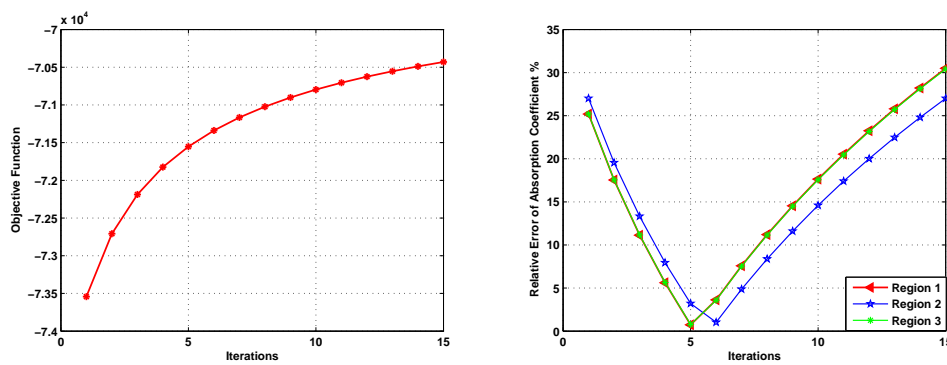

Fig. 5.5. The value of objective function and the relative error of absorption plotted against the iteration. Left: the objective function and right: the relative error of absorption coefficient.

References

[1] J. Beuthan, C. Mahnke, U. Netz, O. Minetb and G. Müller, Optical molecular imaging: Overview and technological aspects,*Medical Laser Application*, **17**:1 (2002), 25–30.

[2] D. Leff, O. Warren, L. Enfield, A. Gibson, T. Athanasiou, D. Patten, J. Hebden, G. Yang and A. Darzi, Diffuse optical imaging of the healthy and diseased breast: A systematic review, *Breast Cancer Research and Treatment*, **108**:1 (2008), 9–22.

[3] S. van de Ven, S. Elias, A. Wiethoff, M. van der Voort, T. Nielsen, B. Brendel, C. Bontus, F. Uhlemann, R. Nachabe, R. Harbers, M. van Beek, L. Bakker, M. van der Mark, P. Luijten and W. Mali, Diffuse optical tomography of the breast: preliminary findings of a new prototype and comparison with magnetic resonance imaging, *European Radiology*, **19**:5 (2009), 1108–1113.

[4] A. Scheel, M. Backhaus, A. Klose, B. Moa-Anderson, U. Netz, K. Hermann, J. Beuthan, G. Muller, G. Burmester and A. Hielscher, First clinical evaluation of sagittal laser optical tomography for detection of synovitis in arthritic finger joints, *Annals of the Rheumatic Diseases*, **64**:2 (2005), 239–245.

[5] T. Austin, A. Gibson, G. Branco, R. Yusof, S. Arridge, J. Meek, J. Wyatt, D. and Delpy and J. Hebden, Three dimensional optical imaging of blood volume and oxygenation in the neonatal brain, *Neuroimage*, **31**:4 (2006), 1426–1433.

[6] H. Dehghani, B. White, B. Zeff, A. Tizzard and J. Culver, Depth sensitivity and image reconstruction analysis of dense imaging arrays for mapping brain function with diffuse optical tomography, *Applied Optics*, **48**:10 (2009), D137–D143.

[7] S. Arridge, Optical tomography in medical imaging, *Inverse Problems*, **15**:2 (1999), R41–R93.

[8] A. Gibson, J. Hebden and S. Arridge, Recent advances in diffuse optical imaging, *Physics in Medicine and Biology*, **50**:4 (2005), R1–R43.

[9] V. Markel and J. Schotland, Inverse problem in optical diffusion tomography. I. Fourier-Laplace inversion formulas, *Journal of the Optical Society of America A. Optics, Image Science, and Vision*, **18**:6 (2001), 1336–1347.

[10] V. Markel and J. Schotland, Inverse problem in optical diffusion tomography. II. Role of boundary conditions, *Journal of the Optical Society of America A. Optics, Image Science, and Vision*, **19**:3 (2002), 558–566.

[11] V. Markel, V. Mital and J. Schotland, Inverse problem in optical diffusion tomography. III. Inversion formulas and singular-value decomposition, *Journal of the Optical Society of America A. Optics, Image Science, and Vision*, **20**:5 (2003), 890–902.

[12] S. Arridge and M. Schweiger, A gradient-based optimisation scheme for optical tomography, *Optics Express*, **2**:6 (1998), 213–226.

[13] C. Wang and M. Jiang, An EM-like optimization scheme for diffuse optical tomography, in *Proceedings of the SPIE - The International Society for Optical Engineering*, 2008, 707608 (12 pp.).

[14] W. Egan, T. Hilgeman and J. Reichman, Determination of absorption and scattering coefficients for nonhomogeneous media.2: Experiment, *Applied Optics*, **12**:8 (1973), 1816–1823.

[15] M. Keijzer, W. Star and P. Storchi, Optical diffusion in layered media, *Applied Optics*, **9**:27 (1988), 820-1824.

[16] K.C. Chang, Methods in Nonlinear Analysis, Springer Monographs in Mathematics, Springer-Verlag, C. H. Morales, 2005.

[17] M. Krasnosel'skiĭ, G. Vaĭnikko, P. Zabreĭko, Ya. Rutitskiĭ, and V. Stetsenko, Approximate solution of operator equations, Translated from the Russian by D. Louvish, Wolters-Noordhoff Publishing, Groningen, 1972.

[18] B. Godunov and P. Zabreiko, Geometric characteristics for convergence and asymptotics of successive approximations of equations with smooth operators, *Studia Mathematica*, **116**:3 (1995), 225–238.

[19] T. Dierkes, O. Dorn, F. Natterer and V. Palamodov, Fréchet derivatives for some bilinear inverse problems, *SIAM Journal on Applied Mathematics*, **62**:6 (2002), 2092–2113.

[20] M. Jiang, T. Zhou, J. Cheng, C. Cong and G. Wang, Image reconstruction for bioluminescence tomography from partial measurement, *Optics Express*, **15**:18 (2007), 11095–11116.

[21] W. Cheong, S. Prahl, and A. Welch, A review of the optical properties of biological tissues, *IEEE Journal of Quantum Electronics*, **26**:12 (1990), 2166–2185.

[22] S. Arridge, J. Kaipio, V. Kolehmainen, M. Schweiger, E. Somersalo, T. Tarvainen and M. Vauhkonen, Approximation errors and model reduction with an application in optical diffusion tomography. *Inverse Problems*, **22**:1 (2006), 175–195.

[23] V. Kolehmainen, M. Schweiger, I. Nissilä, T. Tarvainen, S. Arridge and J. Kaipio, Approximation errors and model reduction in three-dimensional diffuse optical tomography. *Journal of the Optical Society of America A*, **26**:10 (2009) 2257–2268.

[24] T. Elfving and T. Nikazad, Stopping rules for Landweber-type iteration, *Inverse Problems*, **23**:4 (2007), 1417–1432.

[25] Z. Yu and C. Wu and Y. Lin, M. Chuang, J. Tsai and C. Sun, Simultaneous iterative reconstruction technique for diffuse optical tomography imaging: iteration criterion and image recognition, in *Proceedings of the Society of Photo-Optical instrumendtation Engineers (SPIE)*, 2008, 6864 (page 686414).